Received: December 1, 2022. Revised: January 11, 2023.

INASS

International Journal of
Intelligent Engineering & Systems

http://www.inass.org/

A Modified Block Backstepping Controller for Autonomous Vehicle Lane Changing

Mazin Ismael Al-Saedi[1]*

[1]*Technical Instructors Training Institute, Middle Technical University, Baghdad, Iraq*
* Corresponding author's Email: dr.mazin.ismael@mtu.edu.iq

Abstract: In this paper, a modified block backstepping controller was formulated for double lane changing control of a two-degree-of-freedom (2DOF) autonomous vehicle. For a systematic procedure, a 5th-degree polynomial double lane change trajectory was created. Next, the state model dynamics of this underactuated 2DOF autonomous vehicle is presented, which was transformed into the block-strict feedback form. Thereafter, the block backstepping technique was implemented to achieve the control input (steering angle). For enhancing the steady state performance during the trajectory tracking, an integral action was included in the proposed controller. The stability of this controller was established through the Lyapunov theory. To investigate the effectiveness of this proposed controller, we compared it with a human driver's transfer function controller and LQR controller, in addition to the sliding mode controller. Simulation results were achieved using CarSim-Simulink. Later, this controller was implemented to track the same lane change path with a different road coefficient of friction. The supposed controller characteristic was further investigated by inspecting the motion of the vehicle when exposed to an idealized lateral step force disturbance. The simulation results indicated the power of modified block backstepping control and it has higher following accuracy, better yaw rate tracking, and stable front steering angle, at high speed and at high and low friction roads.

Keywords: Block backstepping, Autonomous vehicle, Lane changing, Lyapunov theory, Lateral control, Underactuated mechanism, LQR, Sliding mode.

1. Introduction

In recent years, significant research has been conducted in the field of improving vehicle stability and control. The ultimate targets in automating the driving process are minimizing accidents caused by driver error and improving safety. Simultaneously, the advanced technologies can reduce road congestion and diminish air pollution by reducing fuel consumption and emissions [1]. More than 40% of all traffic accidents between 80 and 100 km/h, according to Audi research, are related to spin out [2]. Attention should be paid by drivers to the surrounding circumstances and other vehicles all the time, and then a corresponding decision should be made immediately, based on the driver's experience and their attention. Drivers' reaction delays lead to road fatalities [3]. Generally, autonomous vehicles can greatly enhance the efficiency of the driving through traffic congestion avoidance, speed maneuvers, and optimal path planning. Based on the deviation between the current position and the desired path, the control system constantly adjusts the steering, wheel angle, and speed until the destination can be reached [3].

Obstacle avoidance, especially lane changing, lane following, or overtaking other vehicles are common driving behaviors in autonomous vehicles. The purpose of a lane change is to pass the front vehicle to reduce driving time, which usually occurs in a situation where the vehicle in front travels slower than the vehicle behind it, and the driving conditions in the adjacent lane are outstanding [3].

Lateral and yaw stability control of the vehicle are considered primary tasks in vehicle dynamics. Lateral dynamic control of vehicles is generally performed by braking and steering subsystems. By

using steering and braking systems [4], the controller must control the yaw rate and sideslip angle to follow the designed path quickly and responsively. Steering control plays an important role in safe driving of the vehicle along the assumed trajectory, and the current paper attempts to shed light on this issue.

By adopting a linear vehicle model of two degrees of freedom (2DOF), the control law can be simplified. The Lyapunov method is a practical technique for feedback controller design. Various methods have been proposed on lane changing for automatic driving technology. The concepts of sliding mode control, based on Lyapunov stability, have been presented in the literature [5]. However, to improve the results of the classical sliding mode controller, many researchers integrated it with different methods, for instance, fuzzy sliding systems [6], adaptive fuzzy systems [7], the proportional integral (PI) controller [8], and fuzzy neural networks (FNNs) [9].

A hierarchical control architecture was proposed by [10] consisting of an upper controller and lower controller. Meanwhile, a Kalman filter-based vehicle sideslip angle observer with a strong tracking theory modification (ST-SRCKF), was established to estimate the sideslip angle. However, in this approach, the implemented adaptive-weight method depends on fuzzy logic control (FLC). Moreover, DYC is needed to outfit the additional yaw moment to guarantee perfect dynamic performance.

The authors in [11] presented a model predictive controller (MPC) for lateral stability control of electric vehicles, while [12] used FLC and the MPC. Based on active front steering (AFS), the authors of [13] consolidated the MPC with RBFNN-PID for parameters tuning. However, this type of the tracking controller suffers from high computations and lack of proof of the stability of the system.

An optimal LQR and PID controller was designed for improving stability, maneuverability, and path tracking for a vehicle model [14]. The deep Q-network (DQN) algorithm [15] has also been proposed. However, these types of algorithms are not suitable to cope with large and/or continuous action spaces [16]. The improved artificial potential field method (APF) [17] suffers from three flaws unless it is combined with machine learning to solve the drawbacks [18].

Lately, various modified backstepping techniques have been designed to extend the advantageous features of the backstepping technique to effectively remedy the control problems of different classes of nonlinear systems and their stabilization problem [19, 20].

Since the nonlinear system is not generally a normal form, normal backstepping control methods cannot be used directly for tracking control of these systems. [21] presented the following observer-based backstepping control method: First, the lateral offset of the current lane as a straight lane for small curvature is approximated. Then, the approximated lateral offset is utilized to obtain the reduced second-order model in the form of strict feedback. Consequently, the backstepping control can be implemented for the reduced model. Finally, an augmented observer is designed to estimate the full state and unknown parameters and external disturbances. Following the same procedure, a backstepping control method with a sliding mode observer was presented in [22] for an autonomous lane-keeping system. The reduced second-order model was proposed for the backstepping control design of the lateral dynamics. In [23] the combination of sliding mode and adaptive backstepping is suggested. Meanwhile, [24] designed a cascaded backstepping control structure comprising an inner-loop electric power steering (EPS) system and an outer-loop lane-keeping system. However, the nonlinearity of the vehicle increased as the radius of curvature decreased. Furthermore, owing to the simplification of the dynamic steering model, there was a disturbance when the vehicle entered or exited the curved road.

A backstepping sliding mode trajectory tracking controller was designed based on the inverted method and sliding mode control by [25]. However, only simulations of a road of a long radius of curvature were conducted. [26] adopted the hierarchical control structure. In the upper controller, to follow the path with high accuracy, the path following error model was converted into the yaw rate tracking problem employing the backstepping approach. Later, the MPC was designed to produce the steering angle and additional yaw moment. In the lower controller, the optimal torque was carried out to provide it to each tire. Noticeably, one of the limitations of the MPC was the large number of short time steps of prediction, leading to computational costs [27]; hence it is difficult to ensure the real-time requirements of the system [28].

The authors in [29] proposed a method consisting of two sliding surfaces. Because the error dynamics is a not-strict feedback system, a brake steer force input was developed to regulate the two sliding surfaces using a backstepping procedure under the driver torque. Despite the simplicity and effectiveness of the DYC, using this differential braking technique resulted in wasting the energy

provided for one of the wheels in the form of heat [30]; furthermore, the control action will cause deceleration of the vehicle [31].

Among the different feedback control techniques, backstepping and sliding mode controllers are dependent on the theory of a Lyapunov function, which guarantees the stability of the system. Based on the integral backstepping controller, coupled longitudinal and lateral motions and the variance of the tracks' curvature was proposed by [32].

However, the trajectory tracking problem of the nontriangular normal form underactuated mechanical systems is still an open research problem [33] because most of the proposed control methods are either non-applicable for real time applications or it have many simplifications.

The block backstepping technique has emerged as one of the most efficient backstepping-based techniques [20]. Based on block backstepping, a tracking controller was developed by [34] for a wheeled mobile robot. Nonetheless, for tracking control problems of more generalized nonlinear dynamic systems, the studied methods cannot be applied directly [19]. A procedure should be devised for the dynamic system to be controlled by modified block backstepping:

1- At the first stage of the design, the system dynamic equations are transformed into a block-strict feedback [19].

2- At the next stage, the backstepping procedure is applied on each dynamic block to obtain the equation of control input for the whole nonlinear system [19].

For improving vehicle stability, many researchers have studied the influence of the driver on the handling controllability, for instance, [35] proposed a PID driver model.

In this research, the lateral dynamics of a vehicle for tracking a desired path is controlled by an adaptive modified block backstepping controller. The 2DOF autonomous vehicle model and lateral position with constant longitudinal speed was implemented. Controller simulation was handled using the connection of CarSim with Simulink. The reference tracking path consisted of a double lane change maneuver. Simulation results indicated a precise tracking contrast to the LQR controller and the human driver's transfer function controller, then a test for the block backstepping controller under a low and high friction driving maneuver.

The main contribution of this paper is to propose a modified block backstepping controller for the nontriangular normal form underactuated autonomous vehicle. There is no need for either an approximation to the polynomial order function of the lane or for an augmented observer. The global stabilization of the model dynamic was ensured by the suggested control law. The proposed controller, LQR controller, and a human driver's transfer function controller, furthermore sliding mode controller, were compared and analyzed by CarSim-Simulink under different coefficients of friction. Moreover, the performance of the proposed controller was tested under a limited disturbance for an autonomous vehicle changing lanes.

The remaining sections of this papers are organized as follows. In section 2 a desired path is described. Section 3 presents the formulation of the dynamics of the 2DOF vehicle model. A systematic derivation of the input control algorithm and the stability of the controller is presented in section 4. The simulation and results are given in section 5, and to the proposed controller is compared to the LQR controller and the human driver's controller in [36]. Finally, section 6 presents conclusions based on the results of this research.

2. Path planning

A 5th-degree polynomial function was implemented in this study for double lane changes, as shown in Fig. 1. Assuming that the state vectors ζ_a and ζ_b are the lateral displacement, velocity, and acceleration of the starting point (i) and the final point (f) for each lane change interval (I and II), respectively, i.e.,

$$\begin{aligned}\zeta_I&=\begin{bmatrix}y_i & \dot{y}_i & \ddot{y}_i & y_f & \dot{y}_f & \ddot{y}_f\end{bmatrix}_I^T\\ \zeta_{II}&=\begin{bmatrix}y_i & \dot{y}_i & \ddot{y}_i & y_f & \dot{y}_f & \ddot{y}_f\end{bmatrix}_{II}^T\end{aligned} \quad (1)$$

Presuming that these initial and final states can be estimated or measured, then a 5th-degree polynomial equation for the path planning can be defined at every time t as

$$y(t) = \sum_{j=0}^{5} a_j t^j \quad (2)$$

where a_j are the coefficients of the polynomial, which can be written as a vector:

$$a = [a_0 \quad a_1 \quad a_2 \quad a_3 \quad a_4 \quad a_5]^T \quad (3)$$

which can be calculated for both 5th-degree polynomial lane intervals as

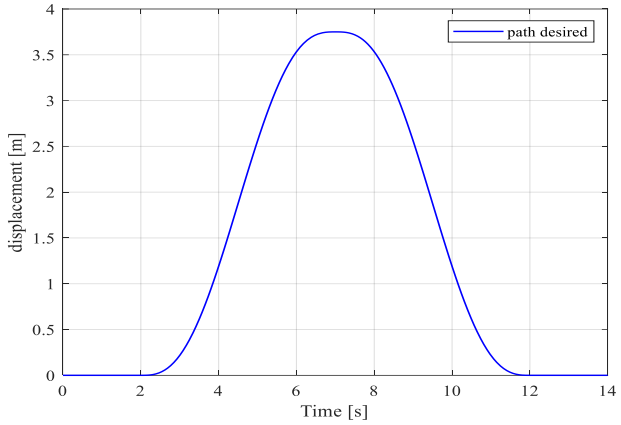

Figure. 1 Desired path (y(t)) for double lane change

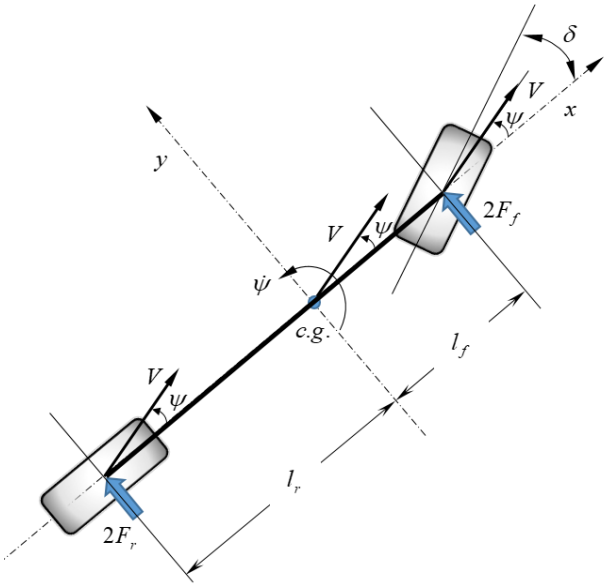

Figure. 2 Dynamics of a 2DOF model of autonomous vehicle

$$a = T^{-1}\zeta \quad (4)$$

where

$$T = \begin{bmatrix} 1 & t_i & t_i^2 & t_i^3 & t_i^4 & t_i^5 \\ 0 & 1 & 2t_i & 3t_i^2 & 4t_i^3 & 5t_i^4 \\ 0 & 0 & 2 & 6t_i & 12t_i^2 & 20t_i^3 \\ 1 & t_f & t_f^2 & t_f^3 & t_f^4 & t_f^5 \\ 0 & 1 & 2t_f & 3t_f^2 & 4t_f^3 & 5t_f^4 \\ 0 & 0 & 2 & 6t_f & 12t_f^2 & 20t_f^3 \end{bmatrix} \quad (5)$$

Then, the desired path can be designed as four intervals: (i) horizontal straight interval (0-2s), (ii) left of 5th-degree polynomial function lane change (2-7s), (iii) right of the 5th-degree polynomial lane change (7-12s), (iv) horizontal straight interval (12-14s). However, the desired yaw angle can be designed as: $\psi_d = \arctan((dy/dt)/V_x)$, where V_x is the x-axis of the velocity as indicated in Fig. 2 [32].

3. Vehicle dynamics

In this study, a simplified 2DOF bicycle model (Fig. 2) for modeling an autonomous vehicle was implemented. According to Newton's second law, the equations of motion along the y-direction and yaw-direction, respectively, are:

$$m\ddot{y} = 2F_f + 2F_r \quad (6)$$

$$I\ddot{\psi} = 2l_f F_f - 2l_r F_r \quad (7)$$

Here, r refers to rear and f front, m is the mass of the vehicle, I is the moment of inertia, l_f and l_r are the distances of the front and rear wheel axles from the center of gravity. Here y represents the vehicle's lateral displacement, and ψ yaw angle. The lateral forces acting on the front and rear wheels, F_f and F_r, respectively, can be reformulated as [36]:

$$F_f = K_f\left(\delta + \psi - \frac{1}{V}\dot{y} - \frac{l_f}{V}\dot{\psi}\right) \quad (8)$$

$$F_r = K_r\left(\psi - \frac{1}{V}\dot{y} + \frac{l_r}{V}\dot{\psi}\right) \quad (9)$$

Where δ is the steering angle, while K_f and K_r represent the front and rear wheel cornering stiffness, respectively. Substituting these variables into Eqs. (6) and (7), and rearranging gives the following:

$$m\ddot{y} = -\frac{2(K_f+K_r)}{V}\dot{y} - \frac{2(l_f K_f - l_r K_r)}{V}\dot{\psi} + 2(K_f + K_r)\psi + 2K_f\delta \quad (10)$$

$$I\ddot{\psi} = -\frac{2(l_f K_f - l_r K_r)}{V}\dot{y} - \frac{2(l_f^2 K_f + l_r^2 K_r)}{V}\dot{\psi} + 2(l_f K_f - l_r K_r)\psi + 2l_f K_f\delta \quad (11)$$

$$\frac{d}{dx}\begin{bmatrix} y \\ \dot{y} \\ \psi \\ \dot{\psi} \end{bmatrix} = \begin{bmatrix} 0 & 1 & 0 & 0 \\ 0 & -\frac{2(K_f+K_r)}{mV} & \frac{2(K_f+K_r)}{m} & -\frac{2(l_f K_f - l_r K_r)}{mV} \\ 0 & 0 & 0 & 1 \\ 0 & -\frac{2(l_f K_f - l_r K_r)}{IV} & \frac{2(l_f K_f - l_r K_r)}{I} & -\frac{2(l_f^2 K_f - l_r^2 K_r)}{IV} \end{bmatrix}\begin{bmatrix} y \\ \dot{y} \\ \psi \\ \dot{\psi} \end{bmatrix} + \begin{bmatrix} 0 \\ \frac{2K_f}{m} \\ 0 \\ \frac{2l_f K_f}{I} \end{bmatrix}\delta \quad (12)$$

Then the dynamic model of the 2DOF autonomous vehicle can be written in a matrix form as

For simplifications, let $x_1 = y$, $x_2 = \psi$, $\dot{x}_1 = \dot{y}$, , $\dot{x}_2 = \dot{\psi}$, and $u = \delta$ then this state model can be written in a reduced form as

$$\begin{aligned} \dot{x}_1 &= x_3 \\ \dot{x}_2 &= x_4 \\ \dot{x}_3 &= A_2x_2 + A_1x_3 + A_3x_4 + A_4u \\ \dot{x}_4 &= B_2x_2 + B_1x_3 + B_3x_4 + B_4u \end{aligned} \quad (13)$$

Rewriting the state variables as follows: $q_1 = x_1, q_2 = x_2, p_1 = x_3, p_2 = x_4, g_1 = A_4$, and $g_2 = B_4$, and rewriting the state model of the 2DOF autonomous vehicle as follows:

$$\begin{aligned} \dot{q}_1 &= p_1 \\ \dot{q}_2 &= p_2 \\ \dot{p}_3 &= f_1(q,p) + g_1(q)u \\ \dot{p}_4 &= f_2(q,p) + g_2(q)u \end{aligned} \quad (14)$$

The state vector can be written as $X = [q_1 \quad q_2 \quad p_1 \quad p_2]^T$.

4. Block backstepping controller design

Because the dynamic model is not in strict feedback form, one cannot apply the method of integrator backstepping control of [37] directly. Consequently, the dynamic model should be first converted into a block-strict feedback form [20].

4.1 The controller design

Step 1: Consider the desired trajectory as: $X_d = [q_{d1} \quad q_{d2} \quad p_{d1} \quad p_{d2}]^T$. Substituting it into Eq. (14) produces

$$\begin{aligned} \dot{q}_{d1} &= p_{d1} \\ \dot{q}_{d2} &= p_{d2} \\ \dot{p}_{d3} &= f_{d1}(q_d,p_d) + g_{d1}(q)u_d \\ \dot{p}_{d4} &= f_{d2}(q_d,p_d) + g_{d2}(q)u_d \end{aligned} \quad (15)$$

Then the tracking error vector can be stated as

$$e = X_d - X = [e_1 \quad e_2 \quad e_3 \quad e_4]^T \quad (16)$$

Differentiation with respect to time on two sides of Eq. (16) gives the error dynamics as

$$\begin{aligned} \dot{e}_1 &= e_3 \\ \dot{e}_2 &= e_4 \\ \dot{e}_3 &= f_{d1}(q_d,p_d) + g_{d1}(q_d)u_d - \\ &\qquad (f_1(q,p) + g_1(q)u) \\ \dot{e}_4 &= f_{d2}(q_d,p_d) + g_{d2}(q_d)u_d - \\ &\qquad (f_2(q,p) + g_2(q)u) \end{aligned} \quad (17)$$

Step 2: Defining an adequate new control variable z_1[34] as

$$z_1 = e_2 - k(e_1 + g_2e_3 - g_1e_4) \quad (18)$$

where k is a design constant. Deriving z_1 with respect to time can be written as

$$\begin{aligned} \dot{z}_1 &= e_4 - k(e_3 + g_2\dot{e}_3 + \dot{g}_2e_3 - g_1e_4 - \dot{g}_1e_4) \\ &= e_4 - k\big(e_3 + g_2\big((f_{d1} + g_{d1}u_d) - (f_1 + g_1u)\big) \\ &\quad + e_3D(g) - g_1\big((f_{d2} + g_{d2}u_d) - (f_2 + g_2u)\big) \\ &\quad - e_4D(g)\big) \end{aligned} \quad (19)$$

where $D(g) = \sum\big(\partial g_{ij}/\partial e_k\big)\,\dot{e}_k$, which maps the time derivative of $g_i(q)$. Since g_i = constant, hence, $D(g) = 0$. For simplification of Eq. (19), let

$$\dot{z}_1 = e_4 - k\Omega \quad (20)$$

Where

$$\begin{aligned} \Omega = e_3 + g_2\big((f_{d1} + g_{d1}u_d) - (f_1 + g_1u)\big) - \\ g_1\big((f_{d2} + g_{d2}u_d) - (f_2 + g_2u)\big) \end{aligned}$$

Step 3: Here, a stabilization function is chosen, which is given as

$$\alpha = -c_1z_1 - \lambda\Gamma + k\Omega \quad (21)$$

where $\Gamma = \int_0^t z_1 dt$ is the integral error, which was added to enhance steady state achievement, and λ and c_1 are positive design constants.

Step 4: The second control variable is defined as z_2 which can be written as

$$z_2 = e_4 - \alpha \quad (22)$$

Substitution Eqs. (21) and (22) into Eq. (23) leads to the dynamics of the first control variable:

$$\dot{z}_1 = e_4 - \alpha - c_1z_1 - \lambda\Gamma \quad (23)$$

or it can be written as

$$\dot{z}_1 = z_2 - c_1z_1 - \lambda\Gamma \quad (24)$$

By deriving Eq. (22), the dynamics of second control variable can be written as

$$\dot{z}_2 = \dot{e}_4 - \dot{\alpha} \tag{25}$$

$$\dot{z}_2 = \dot{e}_4 + c_1\dot{z}_1 + \lambda\dot{\Gamma} - k\dot{\Omega} \tag{26}$$

or in expanding form:

$$\dot{z}_2 = \dot{e}_4 + c_1\dot{z}_1 + \lambda\dot{\Gamma} - k\left(\frac{\partial\Omega}{\partial e_1}\dot{e}_1 + \frac{\partial\Omega}{\partial e_2}\dot{e}_2 + \frac{\partial\Omega}{\partial e_3}\dot{e}_3 + \frac{\partial\Omega}{\partial e_4}\dot{e}_4 + \frac{\partial\Omega}{\partial q_{1d}}\dot{q}_{1d} + \frac{\partial\Omega}{\partial q_{2d}}\dot{q}_{2d} + \frac{\partial\Omega}{\partial q_{3d}}\dot{q}_{3d} + \frac{\partial\Omega}{\partial q_{4d}}\dot{q}_{4d}\right) \tag{27}$$

where the derivatives of Ω with respect to errors are

$$\begin{aligned}
\frac{\partial\Omega}{\partial e_1} &= -g_2\frac{\partial f_1}{\partial e_1} + g_1\frac{\partial f_2}{\partial e_1}\\
\frac{\partial\Omega}{\partial e_2} &= -g_2\frac{\partial f_1}{\partial e_2} + g_1\frac{\partial f_2}{\partial e_2}\\
\frac{\partial\Omega}{\partial e_3} &= 1 - g_2\frac{\partial f_1}{\partial e_3} + g_1\frac{\partial f_2}{\partial e_3}\\
\frac{\partial\Omega}{\partial e_4} &= -g_2\frac{\partial f_1}{\partial e_4} + g_1\frac{\partial f_2}{\partial e_4}
\end{aligned} \tag{28}$$

And with respect to desired states are

$$\begin{aligned}
\frac{\partial\Omega}{\partial q_{1d}} &= g_2\left(\frac{\partial f_{1d}}{\partial q_{1d}} - \frac{\partial f_1}{\partial q_{1d}}\right) - g_1\left(\frac{\partial f_{2d}}{\partial q_{1d}} - \frac{\partial f_2}{\partial q_{1d}}\right)\\
\frac{\partial\Omega}{\partial q_{2d}} &= g_2\left(\frac{\partial f_{1d}}{\partial q_{2d}} - \frac{\partial f_1}{\partial q_{2d}}\right) - g_1\left(\frac{\partial f_{2d}}{\partial q_{2d}} - \frac{\partial f_2}{\partial q_{2d}}\right)\\
\frac{\partial\Omega}{\partial p_{1d}} &= g_2\left(\frac{\partial f_{1d}}{\partial p_{1d}} - \frac{\partial f_1}{\partial p_{1d}}\right) - g_1\left(\frac{\partial f_{2d}}{\partial p_{1d}} - \frac{\partial f_2}{\partial p_{1d}}\right)\\
\frac{\partial\Omega}{\partial p_{2d}} &= g_2\left(\frac{\partial f_{1d}}{\partial p_{2d}} - \frac{\partial f_1}{\partial p_{2d}}\right) - g_1\left(\frac{\partial f_{2d}}{\partial p_{2d}} - \frac{\partial f_2}{\partial p_{2d}}\right)
\end{aligned} \tag{29}$$

Then the actual time derivative of z_2 becomes

$$\dot{z}_2 = \Psi u - \Psi_1 u_d + \lambda z_1 + c_1(z_2 - c_1 z_1 - \lambda\Gamma) - \emptyset \tag{30}$$

Where

$$\Psi = g_2 - k\left(g_1\frac{\partial\Omega}{\partial e_3} + g_2\frac{\partial\Omega}{\partial e_4}\right) \tag{31}$$

$$\Psi_1 = g_{2d} - k\left(g_{1d}\frac{\partial\Omega}{\partial e_3} + g_{2d}\frac{\partial\Omega}{\partial e_4} + g_{1d}\frac{\partial\Omega}{\partial p_{1d}} + g_{2d}\frac{\partial\Omega}{\partial p_{2d}}\right) \tag{32}$$

And

$$\dot{z}_2 = f_2 - f_{2d} - k\left(\frac{\partial\Omega}{\partial e_1}(p_1 - p_{1d}) + \frac{\partial\Omega}{\partial e_2}(p_1 - p_{1d}) + \frac{\partial\Omega}{\partial e_3}(f_1 - f_{1d}) + \frac{\partial\Omega}{\partial e_4}(f_2 - f_{2d}) + \frac{\partial\Omega}{\partial q_{1d}}\dot{q}_{1d} + \frac{\partial\Omega}{\partial q_{2d}}\dot{q}_{2d} + \frac{\partial\Omega}{\partial q_{3d}}\dot{q}_{3d} + \frac{\partial\Omega}{\partial q_{4d}}\dot{q}_{4d}\right) \tag{33}$$

Step 5: The desired dynamics of z_2 can be designed as

$$\dot{z}_2 = -z_1 - c_1 z_2 \tag{34}$$

where the design constant $c_2 > 0$.

As a result, the control input (i.e., front steering angle δ) can be estimated by the equality of Eqs. (30) and (34), as in the following law:

$$u = \delta = \Psi_1 u_d - (1 - c_1^2 + \lambda)z_1 - (c_1 + c_2)z_2 + \lambda c_1\Gamma - \emptyset/\Psi \tag{35}$$

Eventually, the following strict block feedback state of the original error dynamics of the state model of the system in terms of the variables z_1 and z_2 is achieved:

$$\begin{cases}\dot{z}_1 = z_2 - c_1 z_1 - \lambda\Gamma\\ \dot{z}_2 = -z_1 - c_2 z_2\end{cases} \tag{36}$$

4.2 Stability analysis

Lemma 1: *For the 2DOF vehicle model, applying the control law of Eq. (35) can derive it along the continuous desired tracking path.*

Proof: The system of Eqs. (24) and (34) for the closed loop system should prove that it is asymptotically stable. Proposing the following Lyapunov's function, the first step can be verified, as follows:

$$V = \frac{1}{2}z_1^2 + \frac{1}{2}z_1^2 + \frac{1}{2}\lambda\Gamma^2 \tag{37}$$

Deriving Eq. (37) with respect to time and substituting Eqs. (24) and (34) into it and simplifying lead to

$$\dot{V} = z_1\dot{z}_1 + z_2\dot{z}_2 + \lambda\Gamma z_1 = -c_1 z_1^T z_1 - c_2 z_2^T z_2 \le 0 \tag{38}$$

Eq. (38) appears to prove that $V(t) \le V(0)$ is confirmed; therefore Γ, z_1, and z_2 are bounded in addition to $\dot{z}_1$ and $\dot{z}_2$. Deriving Eq. (38) again gives

$$\ddot{V} = -2c_1 z_1^T\dot{z}_1 - 2c_2 z_2^T\dot{z}_2 \tag{39}$$

Because z_1, z_2, $\dot{z}_1$ and $\dot{z}_2$ are bounded, $\ddot{V}$ is bounded also. Applying Barbalat's lemma [38] proves that z_1 and z_2 converge to zero when $t \to \infty$:

Lemma 2: *The trajectory tracking errors of Eq. (16) grantees asymptotically converge to zero when applying the control law with initial conditions* $[q_1(0) \quad q_2(0) \quad p_1(0) \quad p_2(0)]^T$.

Proof: As long as z_1 and z_2 are proved, it converges asymptotically to zero and the gain $k > 0$; hence, Eq. (18) gives

$$\lim_{t\to\infty} e_2 = \lim_{t\to\infty}[k(e_1 + g_2 e_3 - g_2 e_4)] \quad (40)$$

From Eqs. (21) and (22), the following can be achieved:

$$\lim_{t\to\infty} e_4 = \lim_{t\to\infty} \alpha = \lim_{t\to\infty} \Omega = 0 \quad (41)$$

Substituting these results into Eq. (40):

$$e_1 + k g_2 e_3 \to 0 \quad (42)$$

leads to

$$\lim_{t\to\infty} e_1 = \lim_{t\to\infty} e_3 = 0 \quad (43)$$

As a result, the four variables of the tracking error vector of Eq. (16) converge asymptotically to zero. Consequently, the global stabilization of the dynamic of the 2DOF bicycle car model can be ensured by the suggested control law.

5. Simulation and results

In this section, simulations were conducted to verify the proposed block backstepping controller method using the linking of CarSim and Simulink software. The proposed method was applied to drive a 2DOF autonomous vehicle along a desired double lane change tracking path. Simultaneously, the proposed block backstepping controller was compared with a human driver's control [36], and with the traditional LQR controller (Fig. 3) as described in [26] for the same double lane change tracking path. The weighted matrix used in LQR is selected as: Q= *diag*([1,3,1,3]), R= 10.

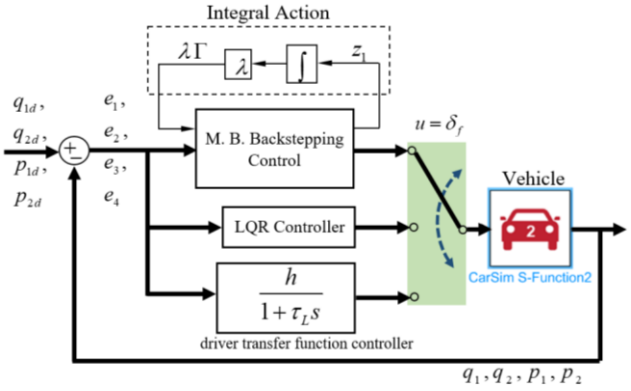

Figure. 3 Schematic diagram of a modified block backstepping, LQR, and driver transfer function controllers for an autonomous vehicle

Table 1. Design parameters of the autonomous vehicle used in this study [36]

Symbol	Parameter	Value
m	Mass	1500 kg
I	Moment of inertia about z-axis	2500 kgm^2
l_f	Distance from C.O.G. to front axle	1.1 m
l_r	Distance from C.O.G. to rear axle	1.6 m
K_f	Front cornering stiffness	55000 N/rad
K_r	Rear cornering stiffness	60000 N/rad
$V = V_x$	Velocity	25 m/s
τ_L	1st order delay time	0.02 sec
h	Proportional gain	0.02 m

Table 2. Manually found parameters of the block backstepping controller

μ	c_1	c_2	λ	k
1	0.01	0.01	0.01	1
0.3	0.01	0.01	0.011	4

The used vehicle model for the simulation is the E - class. The parameters of the vehicle are tabulated in Table 1. Assuming the initial state of the first 5th-degree polynomial function interval is $\zeta_{2\to 7\text{sec}}$=[0 0 0 3.75 0 0] m, and for the second 5th-degree polynomial interval is $\zeta_{7\to 12\text{sec}}$=[3.75 0 0 0 0 0] m.

After mathematical substitution for the current problem, it was easily found that the terms of Eq. (28) are

$$\frac{\partial\Omega}{\partial e_1} = \frac{\partial\Omega}{\partial e_2} = \frac{\partial\Omega}{\partial e_3} = 0, \text{ and } \frac{\partial\Omega}{\partial e_4} = 1$$

which helps in the reduction of Eq. (30).

The design parameters for the block backstepping controller can be selected by trials, as tabulated in Table 2. The numerical value of these parameters should be real and positive to guarantee the stability of the system. The desired control input (u_d) is zero; hence, the required control input (i.e., the steering angle δ) can be written as

$$u = \delta = -(1 - c_1^2 + \lambda)z_1 - (c_1 + c_2)z_2 + \lambda c_1 \Gamma - \emptyset/\Psi \quad (35)$$

The first simulations were conducted under a

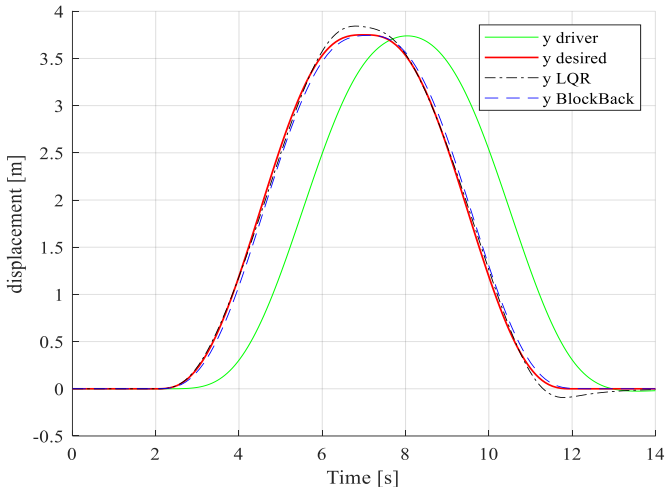

(a)

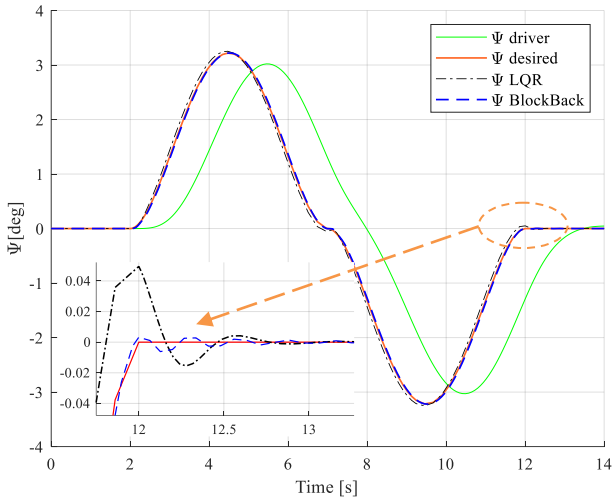

(b)

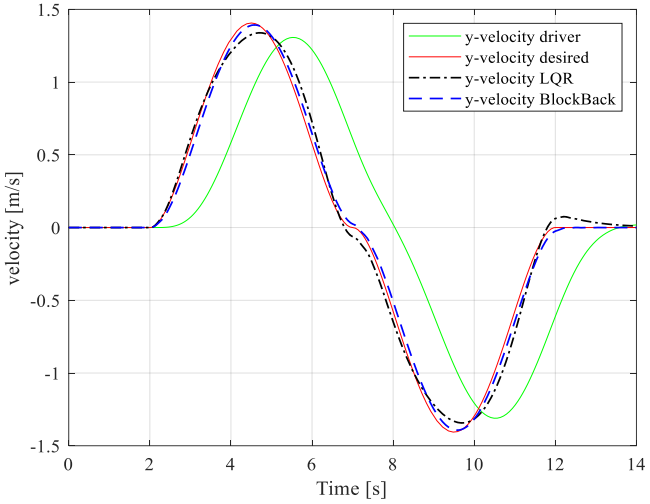

(c)

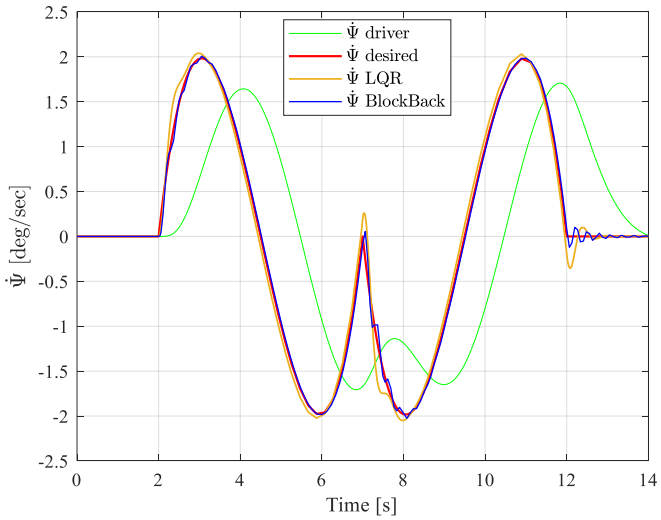

(d)

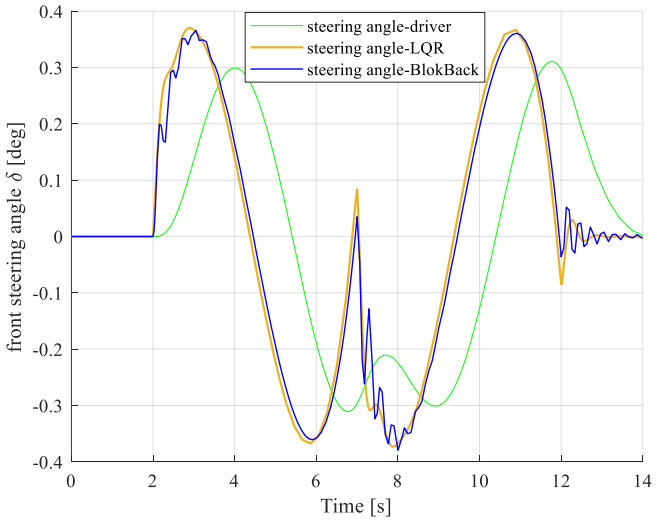

(e)

Figure. 4 Vehicle performance by the suggested block backstepping controller compared to the LQR, and human driver's transfer function controller: (a) displacement, (b) yaw angle, (c) lateral velocity, (d) yaw rate, and (e) front steering angle

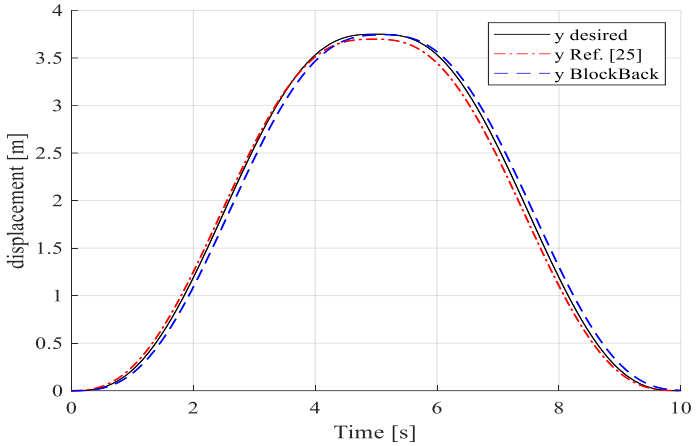

(a)

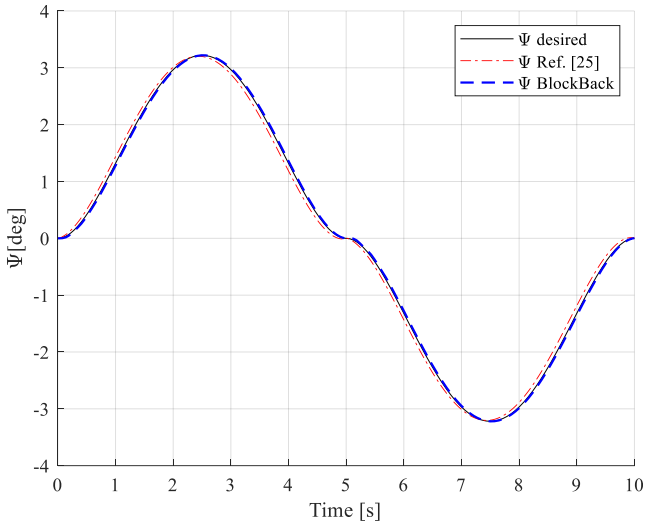

(b)

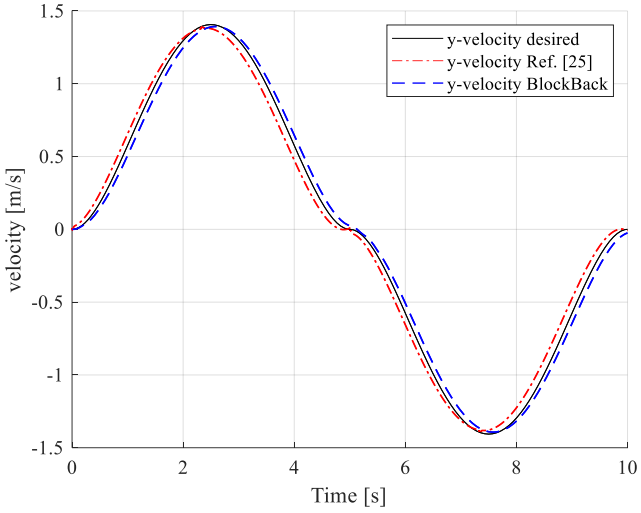

(c)

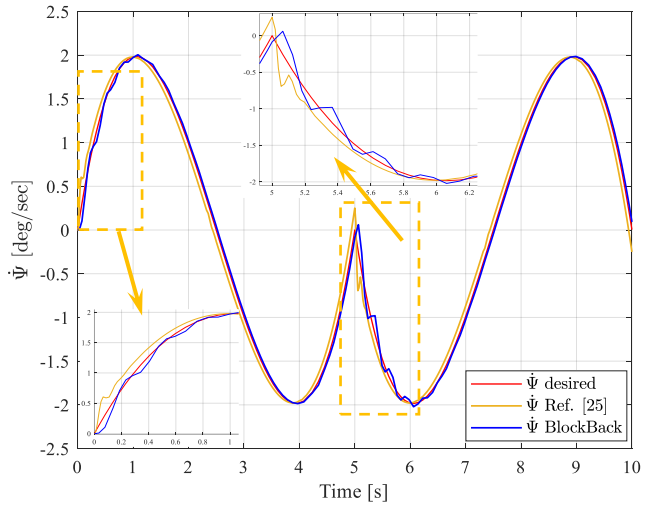

(d)

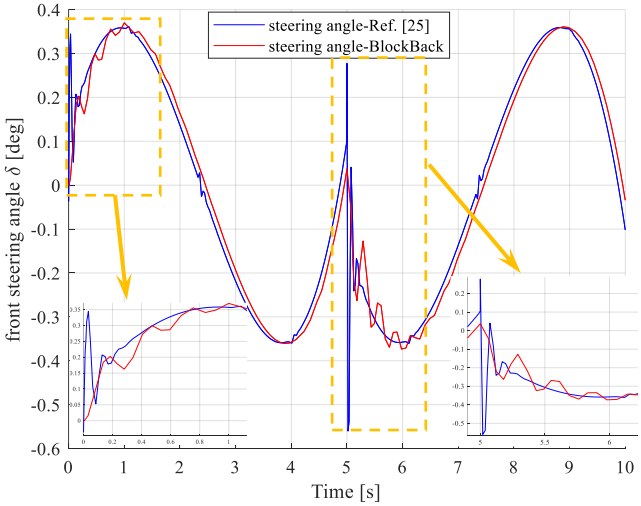

(e)

Figure. 5 Vehicle performance by the suggested block backstepping controller compared to the controller presented by Reference [25]: (a) displacement, (b) yaw angle, (c) lateral velocity, (d) yaw rate, and (e) front steering angle

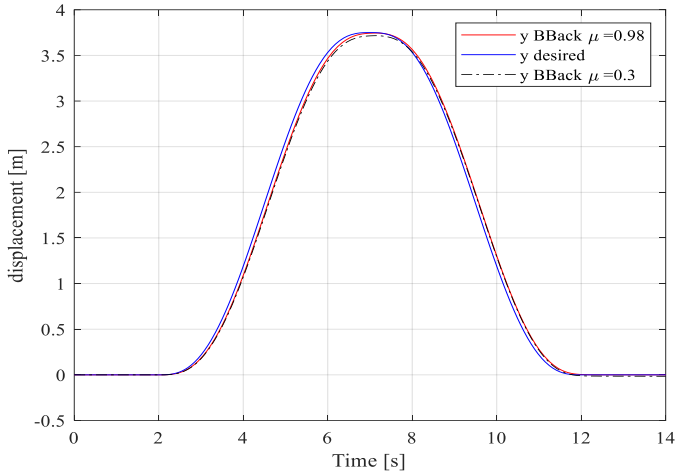

(a)

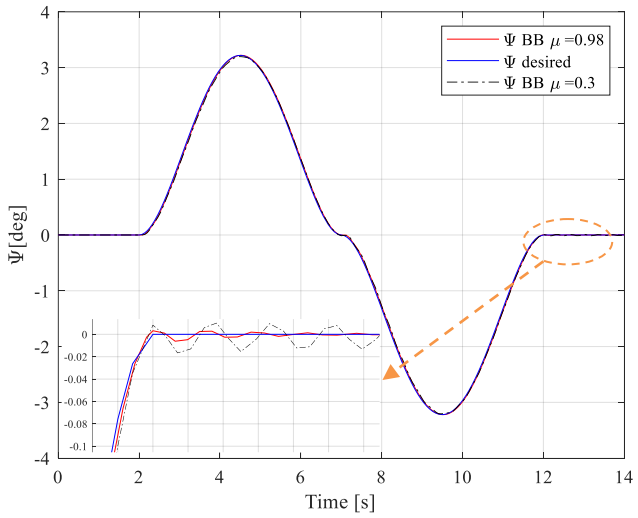

(b)

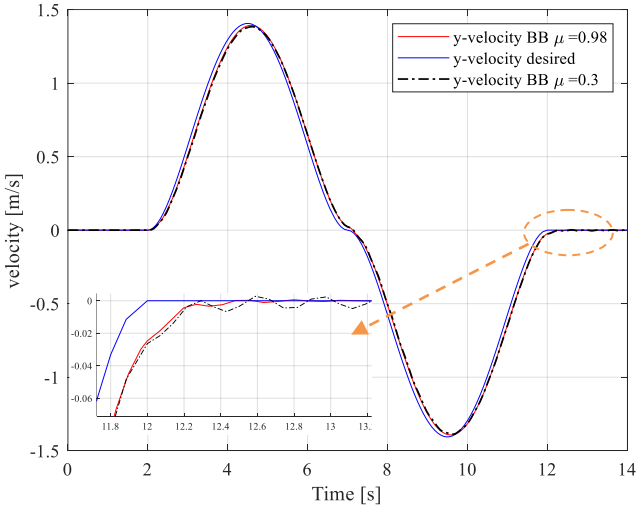

(c)

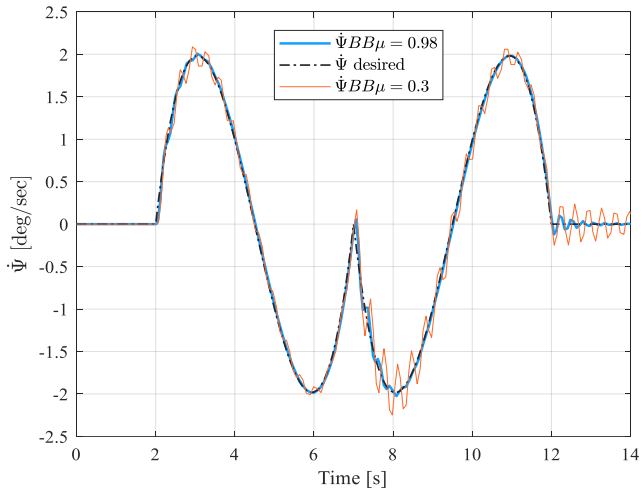

(d)

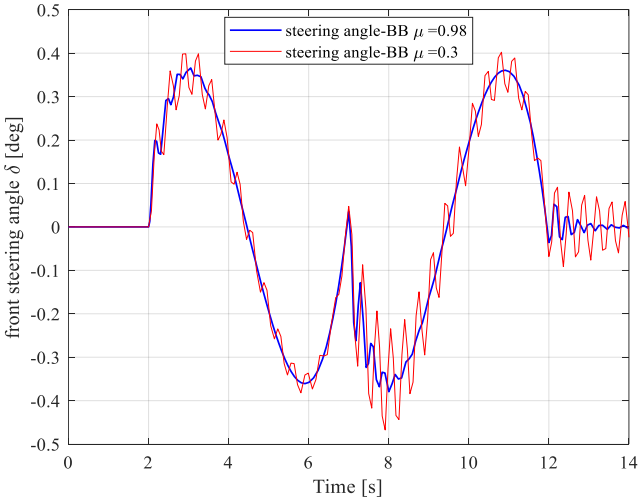

(e)

Figure. 6 Comparison of the suggested block backstepping controller vehicle front steering angle along the desired path for maneuver with $\mu = 0.98$ and $\mu = 0.3$ controllers: (a) Vehicle displacement; (b) Vehicle yaw angle; (c) Vehicle lateral velocity; (d) Vehicle yaw rate; (e) Vehicle front steering angle

constant longitudinal velocity of V=25 m/s, and the coefficient of friction of the road was $\mu = 1$. These simulations for tracking the 2DOF autonomous vehicle in the desired double lane change were conducted using the proposed block backstepping control method. Meanwhile, for comparative purposes, a similar simulation for tracking the 2DOF autonomous vehicle in the desired double lane change were conducted using the LQR controller [26] and the driver transfer function controller method.

Fig. 4 (a) illustrates the lateral displacement of all controllers compared to the reference double lane change tracking path and likewise with respect to yaw angle, lateral velocity, and yaw rate, as can be seen in Fig. 4 (b, c, d) respectively. There is a little difference between the modified block backstepping and LQR controller. However, It can be seen in Fig. 4 (a, b, c, d) that there are a small overshoot with LQR controller at the second part of path.

Additionally, in the case of block backstepping, the front steering angle shown in Fig. 4 (e) followed the desired path in spite of the small vibration during the second lane changing and at the start of the second horizontal tracking path. Consequently, it was clear that the block backstepping controller was stable, and its performance was better than the driver transfer function controller. Clearly, the performance of the block backstepping controller tended to be close to the desired path, while the driver transfer function controller had a delay time and there was a wide difference with respect to the desired path in spite of selecting the optimum τ_L. Fig. 4 (e) shows the simulation result of steering angle (the controller output). Although the steering angle at (7-8) sec and (12-14) sec of the second half of the path using backstepping controller has vibration higher than that the LQR controller, the amplitude of backstepping controller was smaller than the LQR controller and converged quickly.

Both controllers track the desired bath perfectly, but the performance of the modified block backstepping controller in reducing the position and velocity errors is noticeable, which indicates the effectiveness of the proposed controller.

Recent algorithm of [25], which suggested a controller of sliding mode method based on Lyaponov stability condition , is compared to the proposed modified block backstepping method in order to further verify the performance. Using the same vehicle properties of Table 1, and ignoring the wind influence, and implementing the deviation between the actual and the desired yaw angle as the tracking error, i.e., $e_1 = \psi - \psi_d$, and the sliding mode function is defined as

$$s_1 = c_1 e_1 - \dot{e}_1 \tag{44}$$

Defining the control law as in [25] and selecting $\eta_1 = 150$, $\lambda_1 = 5$, $c_1 = 250$, then the front steering angle δ_f can be found to derive the vehicle along double lane change, which defined previously.

Again, under a constant longitudinal velocity of V=25 m/s, and the coefficient of friction of the road was $\mu = 1$, the 2DOF autonomous vehicle in the desired double lane change of 10 sec were simulated using the both methods.

Fig. 5 (a) shows the lane changing trajectory produced by both methods with respect to the desired path, where both of them tracking it without vibrations and the error of block backstepping controller is smaller than Ref. [25] during the interval (5~7)sec. Fig. 5 (b) shows the yaw angle, and clearly that the block backstepping controller is superior than [25]. Meanwhile, Fig. 5 (c) presents the lateral velocity by both methods with respect to the reference velocity.

However, the situations are not the same with respect to the yaw rate and front wheel steering angle where there are vibrations at the beginning of each lane interval as seen in Fig. 5 (d, e), respectively. It can be seen in Fig. 5 (d) that the maximum yaw rate error by using the method of [25] is 0.3511 deg/sec at the first lane, and 0.4757 deg/sec at the second lane (after 5 sec), while the maximum yaw rate error by using the method of block backstepping is 0.2032 deg/sec at the first lane, and 0.1974 deg/sec at the second lane (after 5 sec). Fig. 5 (d) indicates that the maximum front steering angle error by using the method of [25] is 0.3252 deg at the first lane, then goes suddenly at the 5th sec to 0.2772 deg then changes to -0.5599 deg at the 5.019th sec which produces an enormous error of 0.5729 deg then jump up again to +0.0408 deg at the second lane, which is not comfortable driving case along short lane with high speed. Meanwhile the maximum front steering angle error by using the method of block backstepping is 0.0701 deg at the first lane and 0.1083 deg at the second lane (after 5 sec). It can be concluded that both methods can track the trajectory accurately, and the proposed block backstepping controller is superior to [25] in yaw rate and front wheel steering when vehicle travels at high speed and short trajectory.

In the third simulations that were conducted only the proposed block backstepping controller was used with two different coefficients of road friction (μ = 0.98 and μ = 0.3). The longitudinal constant velocity was V=25 m/s. It is worth mentioning here that the

block backstepping parameters (Table 2) should be modified to ensure the stability of the proposed controller and to track the desired path precisely. It is clear from Fig. 6 (a) that the block backstepping controller precisely satisfied the tracking performance of a double lane change reference in cases of both high and low values of friction. This demonstrated the effectiveness of the proposed controller after the correct selection of the controller's parameters. Moreover, this was concluded from the lateral velocity and yaw angle behavior (regardless of the slight ripple along the yaw angle) as in Fig. 6 (b, c) respectively. However, the effect of low friction on the vehicle was clear where there was more vibration than with high friction (Fig. 6 (d)) because of the need for yaw moment to counter the effect of slipping. These sharp vibrations occurred more frequently and were more obvious in the low friction case than in the high friction case, as seen Fig. 6 (e).

All the simulations indicated that the behavior of the suggested modified block backstepping algorithm was stable and could safely drive the vehicle along a desired path with different friction conditions with acceptable stability.

For the controller robustness test, we considered the lateral side wind gust force, Y_w, shown in Fig. 7, acting on the aerodynamic center (AC) of a vehicle moving on a 5th-degree polynomial path. The distance between the AC and the vehicle center of gravity is l_w, and it is positive if the AC is behind the center of gravity [36]. Consequently, the vehicle will deviate from its original path. Hence, the controller should return the vehicle to movement along the path.

If the lateral force, Y_w, and yaw moment N_w, where $N_w = -l_w Y_w$, act on the vehicle, then the equations of motion of the vehicle are rewritten as

$$m\ddot{y} = -\frac{2(K_f + K_r)}{V}\dot{y} - \frac{2(l_f K_f - l_r K_r)}{V}\dot{\psi} + 2(K_f + K_r)\psi + 2K_f\delta + Y_w \quad (45)$$

$$I\ddot{\psi} = -\frac{2(l_f K_f - l_r K_r)}{V}\dot{y} - \frac{2(l_f^2 K_f + l_r^2 K_r)}{V}\dot{\psi} + 2(l_f K_f - l_r K_r)\psi + 2l_f K_f\delta - l_w Y_w \quad (46)$$

We executed a Simulink simulation of the vehicle motion subjected to a wind gust of Y_w = 2.0 kN for a short period (from the 8th sec to the 8.9th sec) $l_w = -0.31$ m (it is negative because the AC is in front of the center of gravity). The vehicle is running at V = 25 m/s and it has the same parameters as in previous simulations.

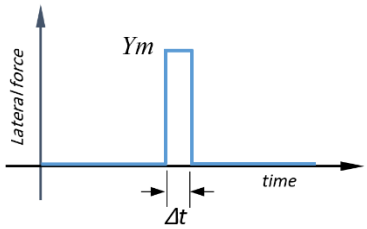

Figure. 7 Lateral side wind gust force

Simulation results for the vehicle subjected to the gust force (from the 8th sec to 8.9th sec) are shown in Fig. 8 (a, b, c). In Fig. 8 (a), it can be seen that the modified block backstepping controller maintained the vehicle moving along the desired path with a deviation not more than 0.11 m, and this was not worse and was acceptable as long as the maneuvering of the car was 3.75 m during a speed of 90 km/h (25 m/s). Clearly, the effect of this disturbance gust force was seen in the velocity and yaw rate curves compared with the same motion without this disturbance gust force (Fig. 8 (b, c)).

Although there was a vibration during the disturbance period, the controller damped it gradually, and the vehicle motion became stable again. Hence, one can perceive the robustness of the suggested control of the study.

6. Conclusions and recommendations

In this research, a double lane change desired track utilizing a 5th-degree polynomial was generated. A block backstepping controller was implemented for tracking the desired path of a 2DOF autonomous vehicle. The state model of this underactuated system was converted into block strict feedback form. Later, a modified block backstepping input control law was formulated. To enhance the tracking control performance, an integral action was combined. The global asymptotic stability of this presented controller was proved by the Lyapunov theory and Barbalat's lemma.

Simulation outcomes (using the CarSim-Simulink Connection) demonstrated the effectiveness of this suggested block backstepping algorithm compared to the controller designed for the LQR controller and the human driver's transfer function as well as sliding mode controller. Furthermore, the controller maintained the vehicle stability in spite of different surfaces or disturbance forces over short periods.

Eventually, finding the optimal constants of the modified block backstepping controller was achieved by trial and error. In upcoming research, a computational method that optimizes these constants,

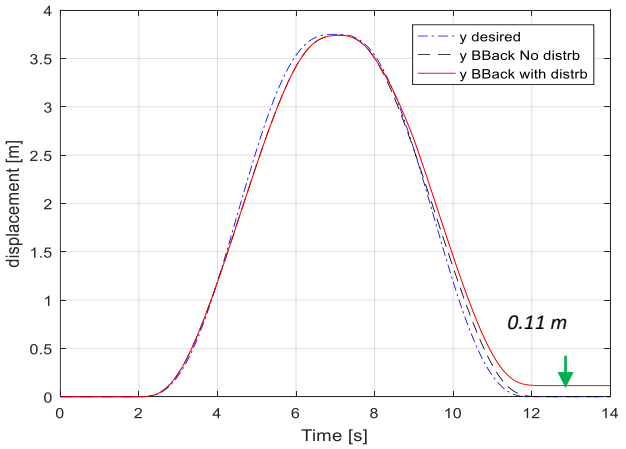

(a)

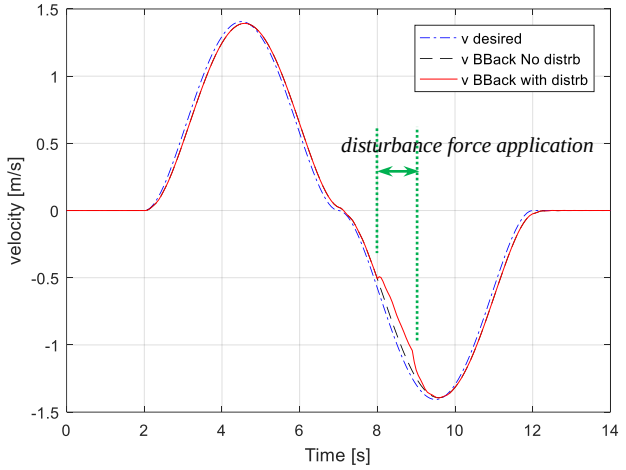

(b)

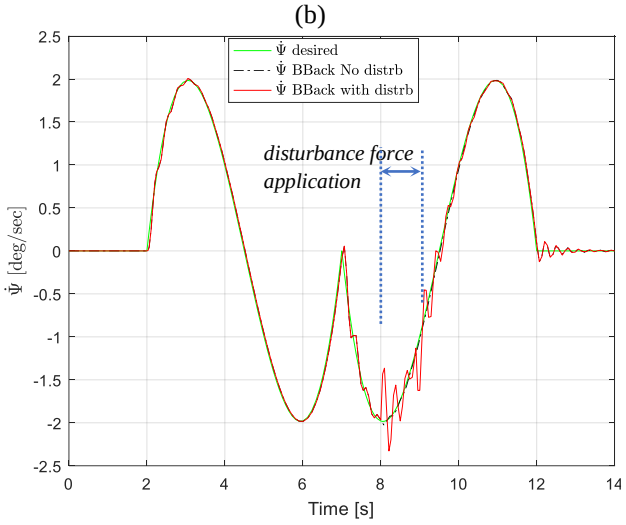

(c)

Figure. 8 Simulation results for the 2DOF vehicle model path tracking controller with and without disturbance: (a) Displacement; (b) Velocity; (c) Yaw rate

for instance, particle swarm optimization (PSO), will be used to improve the candidate controller.

Conflicts of interest

The author declares no conflict of interest.

Author contributions

Conceptualization, M.I.A.; methodology, M.I.A.; software, M.I.A.; validation, M.I.A.; formal analysis, M.I.A.; investigation, M.I.A.; resources, M.I.A.; data curation, M.I.A.; writing—original draft preparation, M.I.A.; writing—review and editing, M.I.A.; visualization, M.I.A.; funding acquisition, M.I.A.

Notations

Symbol	Parameter
ζ_I and ζ_{II}	The state vectors of lateral displacement , velocity, and acceleration for each lane change interval (I and II)
(i) and (f)	The starting point and the final point
a_j	The coefficients of the polynomial
m	Mass of vehicle
I	Moment of inertia about z-axis
f and r	front and rear
l_f	Distance from C.O.G. to front axle
l_r	Distance from C.O.G. to rear axle
K_f, K_r	Cornering stiffness of (front, rear) tires
F_f and F_r	The lateral forces acting on the front and rear wheels
t	time
u	Input control signal
$V = V_x$	Velocity
y	The vehicle's lateral offset
ψ	Yaw angle
δ	The steering angle
X	The state vector in a rewritten form
X_d	The desired trajectory
$e_1 = y - y_d = p_1 - p_{1d}$	lateral offset error
$e_2 = \psi - \psi_d = p_2 - p_{2d}$	yaw angle error
k, λ, c_1, and c_2	Positive design constants
z_1, z_2	The first control variable and The second control variable
τ_L	1st order delay time
h	Proportional gain
μ	Coefficient of road friction
Q and R	Weighted matrix used in LQR

References

[1] P. Petrov and F. Nashashibi, "Modeling and nonlinear adaptive control for autonomous

vehicle overtaking", *IEEE Transactions on Intelligent Transportation Systems*, Vol. 15, pp. 1643-1656, 2014.

[2] D. W. Pi, W. Dong, and X. H. Wang, "Comparing sliding-mode control and PID approaches for vehicle stability control", *Applied Mechanics and Materials*, 2014, pp. 321-326.

[3] S. Xing and M. Jakiela, "Lane change strategy for autonomous vehicle", *Dept. Mech. Eng. Mater. Sci., Washington University in St. Louis, St. Louis*, MO, USA, Tech. Rep. 61, 2018, doi: 10.7936/qn21-9589.

[4] M. K. Aripina, Y. M. Samb, A. D. Kumeresanb, M. F. Ismailc, and P. Kemaod, "A review onintegrated active steering and braking control for vehicle yaw stability system," *Journal Technology*, Vol. 71, No. 2, pp. 105-111, 2014.

[5] J. Lei, H. Wu, J. Yang, and J. Zhao, "Sliding mode lane keeping control based on separation of translation and rotation movement", *Optik*, Vol. 127, pp. 4369-4374, 2016.

[6] L. Li, J. Lian, M. Wang, and M. Li, "Fuzzy sliding mode lateral control of intelligent vehicle based on vision", *Advances in Mechanical Engineering*, Vol. 5, p. 216862, 2013.

[7] J. Guo, L. Li, K. Li, and R. Wang, "An adaptive fuzzy-sliding lateral control strategy of automated vehicles based on vision navigation", *Vehicle System Dynamics*, Vol. 51, pp. 1502-1517, 2013.

[8] H. Alipour, M. B. B. Sharifian, and M. Sabahi, "A modified integral sliding mode control to lateral stabilisation of 4-wheel independent drive electric vehicles", *Vehicle System Dynamics*, Vol. 52, pp. 1584-1606, 2014.

[9] L. Li, H. Wang, J. Lian, X. Ding, and W. Cao, "A lateral control method of intelligent vehicle based on fuzzy neural network", *Advances in Mechanical Engineering*, Vol. 7, p. 296209, 2015.

[10] H. Wang, B. Liu, and J. Qiao, "Advanced High-Speed Lane Keeping System of Autonomous Vehicle with Sideslip Angle Estimation", *Machines*, Vol. 10, p. 257, 2022.

[11] B. Huang, S. Wu, S. Huang, and X. Fu, "Lateral stability control of four-wheel independent drive electric vehicles based on model predictive control", *Mathematical Problems in Engineering*, Vol. 2018, 2018.

[12] J. Wang, F. Teng, J. Li, L. Zang, T. Fan, J. Zhang, and X. Wang, "Intelligent vehicle lane change trajectory control algorithm based on weight coefficient adaptive adjustment", *Advances in Mechanical Engineering*, Vol. 13, p. 16878140211003393, 2021.

[13] Z. He, L. Nie, Z. Yin, and S. Huang, "A two-layer controller for lateral path tracking control of autonomous vehicles", *Sensors*, Vol. 20, p. 3689, 2020.

[14] N. Tavan, M. Tavan, and R. Hosseini, "An optimal integrated longitudinal and lateral dynamic controller development for vehicle path tracking", *Latin American Journal of Solids and Structures*, Vol. 12, pp. 1006-1023, 2015.

[15] L. Yi, "Lane change of vehicles based on DQN", In: *Proc of 2020 5th International Conference on Information Science, Computer Technology and Transportation (ISCTT)*, 2020, pp. 593-597.

[16] F. L. Vincent, H. Peter, I. Riashat, G. B. Marc, and P. Joelle, *An Introduction to Deep Reinforcement Learning*: now, 2018.

[17] H. Hongyu, Z. Chi, S. Yuhuan, Z. Bin, and G. Fei, "An improved artificial potential field model considering vehicle velocity for autonomous driving", *IFAC-PapersOnLine*, Vol. 51, pp. 863-867, 2018.

[18] Z. Yan, L. Jiang, and D. Wu, "A Path Planning Algorithm based on Artificial Potential Field Method and Ant Colony Algorithm", In: *Proc. of 2021 IEEE International Conference on Mechatronics and Automation (ICMA)*, 2021, pp. 1454-1459.

[19] S. Rudra, R. K. Barai, and M. Maitra, "Nonlinear state feedback controller design for underactuated mechanical system: A modified block backstepping approach", *ISA Transactions*, Vol. 53, pp. 317-326, 2014.

[20] S. Rudra, R. K. Barai, and M. Maitra, *Block Backstepping Design of Nonlinear State Feedback Control Law for Underactuated Mechanical Systems*: Springer, 2017.

[21] C. M. Kang, W. Kim, and C. C. Chung, "Observer-based backstepping control method using reduced lateral dynamics for autonomous lane-keeping system", *ISA Transactions*, Vol. 83, pp. 214-226, 2018.

[22] C. M. Kang, W. Kim, S. H. Lee, and C. C. Chung, "Backstepping Control Method with Sliding Mode Observer for Autonomous Lane Keeping System", *IFAC-PapersOnLine*, Vol. 50, pp. 6989-6995, 2017.

[23] W. Kim, C. M. Kang, Y. S. Son, and C. C. Chung, "Nonlinear backstepping control design for coupled nonlinear systems under external disturbances", *Complexity*, Vol. 2019, 2019.

[24] C. M. Kang, W. Kim, and H. Baek, "Cascade backstepping control with augmented observer for lateral control of vehicle", *IEEE Access*, Vol. 9, pp. 45367-45376, 2021.
[25] P. Feng, H. Jin, L. Zhao, and M. Lu, "Active Lane-Changing Control of Intelligent Vehicle on Curved Section of Expressway", *Modelling and Simulation in Engineering*, Vol. 2022, 2022.
[26] C. Wang, R. He, Z. Jing, and S. Chen, "Coordinated Path Following Control of 4WID-EV Based on Backstepping and Model Predictive Control", *Energies*, Vol. 15, p. 5728, 2022.
[27] M. Kim, D. Lee, J. Ahn, M. Kim, and J. Park, "Model predictive control method for autonomous vehicles using time-varying and non-uniformly spaced horizon", *IEEE Access*, Vol. 9, pp. 86475-86487, 2021.
[28] X. Li, N. Xie, and J. Wang, "A variable weight adaptive cruise control strategy based on lane change recognition of leading vehicle", *Automatika*, Vol. 63, pp. 555-571, 2022.
[29] Y. S. Son and W. Kim, "Nonlinear Differential Braking Control for Collision Avoidance During Lane Change", *Mathematics*, Vol. 9, p. 1699, 2021.
[30] N. L. Azad, "Dynamic Modelling and Stability Controller Development for Articulated Steer Vehicles", *Ph.D. dissertation, University of Waterloo*, Waterloo, Ontario, Canada, 2007.
[31] H. Termous, H. Shraïm, R. Talj, C. Francis, and A. Charara, "Coordinated control strategies for active steering, differential braking and active suspension for vehicle stability, handling and safety improvement", *Vehicle System Dynamics*, Vol. 57, pp. 1494-1529, 2019.
[32] L. Guo, P. S. Ge, M. Yue, and Y. B. Zhao, "Lane changing trajectory planning and tracking controller design for intelligent vehicle running on curved road", *Mathematical Problems in Engineering*, Vol. 2014, 2014.
[33] M. R. M. B. Olyaei, A. Ghanbari, and J. Keighobadi, "Trajectory tracking control of a class of underactuated mechanical systems with nontriangular normal form based on block backstepping approach", *Journal of Intelligent & Robotic Systems*, Vol. 96, pp. 209-221, 2019.
[34] S. Rudra, R. K. Barai, and M. Maitra, "Design and implementation of a block-backstepping based tracking control for nonholonomic wheeled mobile robot", *International Journal of Robust and Nonlinear Control*, Vol. 26, pp. 3018-3035, 2016.
[35] S. Yu, W. Li, W. Wang, and T. Qu, "Nonlinear control of active four wheel steer-by-wire vehicles", *IEEE Access*, Vol. 7, pp. 127117-127127, 2019.
[36] M. Abe, *Vehicle Handling Dynamics: Theory and Application*: Butterworth-Heinemann, 2015.
[37] M. Krstic, P. V. Kokotovic, and I. Kanellakopoulos, *Nonlinear and Adaptive Control Design*: John Wiley & Sons, Inc., 1995.
[38] Nikravesh. S. K. Y, *Nonlinear Systems Stability Analysis: Lyapunov-based Approach*, CRC Press: 2018.